Functional Characterization of Ribozymes Expressed Using U1 and T7 Vectors for the Intracellular Cleavage of ANF mRNA†

Mary Beth De Young,‡,§ Julie Kincade-Denker,‡ Cynthia A. Boehm,‡ R. Peter Riek,‡ J. Anthony Mamone,∥ James A. McSwiggen,∥,⊥ and Robert M. Graham*,‡

Department of Cardiovascular Biology, Cleveland Clinic Research Institute, Cleveland, Ohio 44195, and United States Biochemicals, Cleveland, Ohio 44128

Received May 4, 1994; Revised Manuscript Received July 8, 1994®

ABSTRACT: Hammerhead ribozymes targeted to various GUC or GUA sites on rat atrial natriuretic factor (ANF) mRNA were developed. The catalytic activity of ribozymes to four of these sites, synthesized by transcription off synthetic oligodeoxynucleotide duplexes, was studied in detail. *In vitro*, ribozyme-mediated cleavage was highly Mg^{2+}-dependent, and at concentrations approaching those found intracellularly, the rate but not the extent of cleavage was markedly reduced. To test for cellular activity, synthetic genes encoding the ribozymes were cloned between the initiation and termination sequences of the U1snRNA gene or between the T7RNA polymerase promoter and terminator sequences in pSP64. Both constructs had defined initiation and termination sequences to minimize transcript size and for message stability. *In vitro* the addition of T7 or U1 terminator sequences had variable effects on catalytic activity, presumably due to structural interactions between the ribozyme and the added sequence. The ribozyme-encoding plasmids were cotransfected with an expression plasmid containing a rat ANF cDNA into COS-1 cells using a liposome method, which provided high-level transfection efficiency. Quantitation of ANF mRNA by RNase protection showed marked decreases in ANF transcript levels with both the U1- and the T7-expressed ribozymes directed at three of the four sites on ANF mRNA. With all constructs, target accessibility, determined *in vitro*, was a more important determinant of intracellular ANF mRNA cleavage than catalytic activity per se. ANF mRNA cleavage was not merely due to an antisense effect, since a mutant construct that was catalytically inactive but could still bind produced less cleavage than the corresponding wild-type ribozyme construct. These findings indicate that both U1 and T7 vector systems provide efficient ribozyme expression for the intracellular cleavage of target mRNA.

Atrial natriuretic factor (ANF) is a peptide hormone synthesized by atrial cardiomyocytes (Wildey et al., 1992; Rosenzweig & Seidman, 1991). It is released from the heart in response to an increased volume load and other stimuli. Physiological responses to elevated levels include vasorelaxation; diuresis; natriuresis; suppressed secretion of renin, vasopressin, and aldosterone, and suppression of responses to endothelin (Wildey et al., 1992; Rosenzweig & Seidman, 1991; Blaine, 1990). Despite extensive information concerning the acute biological responses to ANF, its role as a long-term physiological regulator of sodium excretion and body fluid homeostasis remains controversial (Blaine, 1990; Goetz, 1990). The concept that ANF is an important regulator of cardiovascular homeostasis is supported indirectly by the finding that its gene structure is highly conserved in evolutionarily diverse species; by correlations between increased plasma ANF levels and the induction of ANF mRNA expression in situations of volume overload, such as congestive heart failure; and by the finding of hypotension in transgenic animals with high circulating ANF levels due to overexpression of the ANF gene (Steinhelper et al., 1990). However, conflicting results have been reported regarding the effect of chronic ANF administration (5–7 days) on arterial blood pressure and natriuresis, and under certain circumstances, natriuresis does not occur even in the presence of high circulating ANF levels (Blaine, 1990; Goetz, 1990).

For these reasons, we sought an approach that would allow inactivation of ANF gene expression in a species such as the rat, which is amenable to detailed physiological study. Ribozymes, which selectively cleave mRNA targets, provide such an approach. Moreover, ANF is potentially a suitable target for inactivation, since regulation of ANF transcription is a major mechanism for modulating hormone production, and peptide levels parallel mRNA abundance (Rosenzweig & Seidman, 1991). Also, the transcript for ANF is relatively short, which may limit the complexity of its tertiary structure, and its mRNA is not G-C rich, which may limit target-site accessibility.

Ribozyme sequences are derived from naturally occurring structures involved in self-cleavage reactions in virioids, virusoids, and linear satellite RNAs (Symons, 1989). The hammerhead ribozyme motif (Haseloff & Gerlach, 1988) used in this study consists of a catalytic "core" sequence, with hybridizing regions (arms) on either side to confer substrate specificity (Figure 1a). Hybridization alone may result in antisense RNA activity, with the added benefit of direct RNA cleavage by the ribozyme. Difficulties encountered in the application of ribozyme technology for the cleavage of cellular targets include the problems intrinsic to antisense RNA

† Supported in part by Grant HL33713 from the National Institutes of Health (R.M.G.), a fellowship (M.B.D.Y.) from the American Heart Association, Northeast Ohio Affiliate, and an Eccles Award (R.M.G.) from the National Health and Medical Research Council, Australia.

* To whom correspondence should be addressed at The Victor Chang Cardiac Research Institute, St. Vincent's Hospital, Darlinghurst 2010, Sydney, N.S.W., Australia (FAX 61-2-361-2922).

‡ Cleveland Clinic Research Institute.

§ Present address: Department of Biological Sciences, 319 Montgomery Hall, Northern Illinois University, DeKalb, IL 60115.

∥ United States Biochemicals.

⊥ Present address: Ribozyme Pharmaceuticals, Inc., Boulder, CO 80301.

® Abstract published in *Advance ACS Abstracts,* September 1, 1994.

0006-2960/94/0433-12127$04.50/0

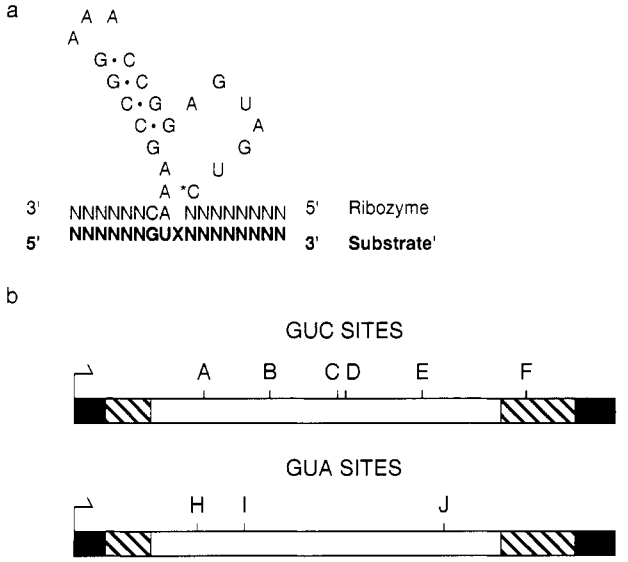

FIGURE 1: (a) Structure of the hammerhead ribozyme and substrate used in these studies. Cleavage of substrate occurs 3′ of the GUX sequence. N is any base, and X is C or A. The numbering system of Hertel et al. (1992) was used, where the first nucleotide (C) of the catalytic core (indicated by the asterisk) is number 3, and the subsequent nucleotides are numbered successively 4–9, 10.1–10.4, L2.1–L2.4, 11.4–11.1, 12, 13, 14. (b) Location of GUC and GUA sites on rANF cDNA. The black regions indicate the polylinker of pBluescript KS; the hatched regions, the 5′ and 3′ untranslated regions; and the open region, the ANF coding region. Arrows indicate the transcription start sites.

technology, such as poor access to highly structured or protein-bound target sites on the mRNA, the challenge of expressing sufficient amounts within cells for maximum activity, and instability of the expressed RNA within cells. Thus, ribozymes that are catalytically active *in vitro*, and are expressed in large amounts, may be inactive in cells (Mazzolini et al., 1992); promoter strength can influence the effectiveness of ribozymes (Cameron & Jennings, 1989; Yu et al., 1993), and unmodified ribozymes may be unstable both in cells (Sioud et al., 1992) and in serum (Yuyama et al., 1992). Additionally, strategies that improve ribozyme expression and stability may interfere with catalytic activity. For example, Chen et al. (1992) reported that a ribozyme expressed as part of a 3-kb transcript to protect it from RNases was inactive, and Yu et al. (1992) indicated that an anti-HIV hairpin ribozyme, with several hundred bases of noncomplementary 5′ flanking sequence, had poor catalytic activity. Furthermore, Yuyama et al. (1992) have reported decreased activity when ribozymes are embedded in a tRNA, although Dropulic et al. (1993) have indicated that increasing the length of the 3′ flanking sequence of a ribozyme to 850 bases had no effect on activity. The activity assay used in this latter study (Dropulic et al.), however, involved initial incubation of ribozyme and substrate at 65 °C, which may have diminished structural interferences and augmented annealing of ribozyme and substrate.

We report here the use of U1 and T7 vector systems to direct the expression of ribozyme constructs of limited and defined size that are sufficiently stable to efficiently cleave ANF mRNA in cells. These vector systems not only may be useful for functional studies of ANF *in vivo* but should be applicable to the selective suppression of other desired genes, either for physiological studies or for therapeutic purposes.

MATERIALS AND METHODS

RNase H Cleavage Assay for Determining mRNA Target Accessibility. The cDNA for rat ANF beginning at base 69

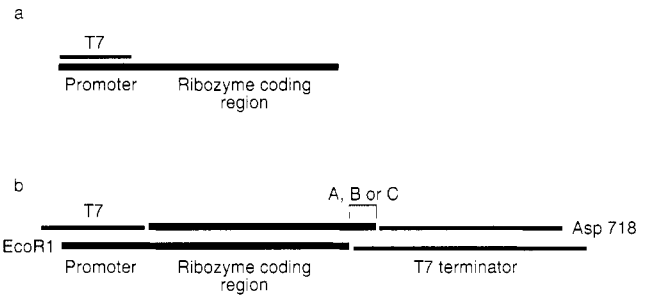

FIGURE 2: (a) Design of the synthetic oligonucleotide duplex for synthesis of ribozymes by *in vitro* transcription with T7 polymerase. (b) Design of the synthetic oligodeoxynucleotide casette for cloning into the *Eco*RI/Asp 718 sites of pSP64. The linker region between the 3′ end of the ribozyme and the T7 terminator is indicated by the bracket. Three different linkers (A–C) were used, as detailed in Materials and Methods.

of the native sequence, which is 12 bases before the translation start site (Seidman et al., 1984), was cloned into the *Eco*RI and *Pst*I sites of pBluescript KS (Stratagene, La Jolla, CA). The plasmid was cleaved at the *Bam*HI site following the cDNA, to give a defined transcript end, and transcribed in the sense direction with T3 RNA polymerase. A MaxiScript transcription kit was used for RNA synthesis (Ambion, Texas) with [α-^{35}S]ATP added for internal labeling.

Oligodeoxynucleotide sequences complementary to sites on ANF mRNA containing GUC or GUA sequences were synthesized on a Milligen/Biosearch 8700 DNA synthesizer (Millipore, Redford, MA) according to standard procedures, and gel purified. The GUC sites were designated A through F, and the GUA sites were designated H through J (Figure 1b). The sequences of the oligodeoxynucleotides synthesized to be complementary to each of these sites, from 5′ to 3′, were as follows: A, TGTTGGACACC; B, GGCATGACCTC; C, GGGTTGACTTC; D, TCTGAGACGGG; E, AGCTTGACCTT; F, CTGTGTGACACA; H, CTGTATACGGG; I, TCTTCTACCGG; and J, AATCCTACCCC. Accessibility of an additional site (X), corresponding to the translation start site, was also evaluated with the following oligodeoxynucleotide: 5′-AAGGAGCCCAT-3′.

The ^{35}S-labeled full-length ANF transcript (92 fmol) and one of each of the oligodeoxynucleotides (46 pmol) were incubated at 37 °C with 0.8 unit of RNase H (Boehringer Mannheim) in 10 μL of a buffer containing 100 mM KCl, 10 mM $MgCl_2$, 0.1 mM EDTA, 1 mM DTT, and 20 mM Tris-HCl, pH 8.0. RNase H cleavage of the ANF transcript at sites bound by the oligodeoxynucleotides was complete by 30 min. The reaction was stopped by addition of 0.5 vol of formamide-containing stop solution (95% formamide, 20 mM EDTA, and 0.5% bromophenol blue). Reaction products were resolved on a 6% polyacrylamide gel containing 7 M urea, visualized by autoradiography, and quantitated using a Molecular Dynamics PhosphorImager (Sunnyvale, CA).

Oligonucleotide Duplexes for Ribozyme Transcription. Oligodeoxynucleotides were synthesized and purified as before. For evaluation of ribozyme activity *in vitro*, ribozymes were transcribed from synthetic duplexes (Figure 2a). The oligonucleotide for the top (noncoding) strand was complementary to the T7 promoter. This oligonucleotide was annealed at the 3′ end to a bottom strand oligonucleotide encoding the T7 promoter (5′-TATAGTGAGTCGTATT-3′) followed by the ribozyme-encoding region. In some cases a C or CG sequence was added at the beginning of the ribozyme-encoding sequence to allow T7 polymerase-mediated transcription at required GG, GA, or GC sequences (Milligan et al., 1987).

Table 1: Ribozyme Coding Strand Sequences

ANFmRNA target site	3′ arm	catalytic core	5′ arm[a]
B	UGAGGU	UUCGGCCUUUCGGCCUCAUCAG	AUGCC
F	GUGUGU	UUCGGCCUUUCGGCCUCAUCAG	ACACAG*C*
H	UCCCGU	UUCGGCCUUUCGGCCUCAUCAG	UACAGU*G*
I	GCCGGU	UUCGGCCUUUCGGCCUCAUCAG	GAAGAU*C*
I_{U7C}	GCCGGU	UUCGGCCUUUCGGCCUC*G*UCAG	GAAGAU*C*
$I_{U7C,G5C}$	GCCGGU	UUCGGCCUUUCGGCCUC*GUGA*G	GAAGAU*C*
J	GGGGU	UUCGGCCUUUCGGCCUCAUCAG	GGAUUGA*GC*

[a] Bases underlined were added to improve transcription with T7 polymerase; bases italicized were altered as shown to give the mutant ribozymes indicated.

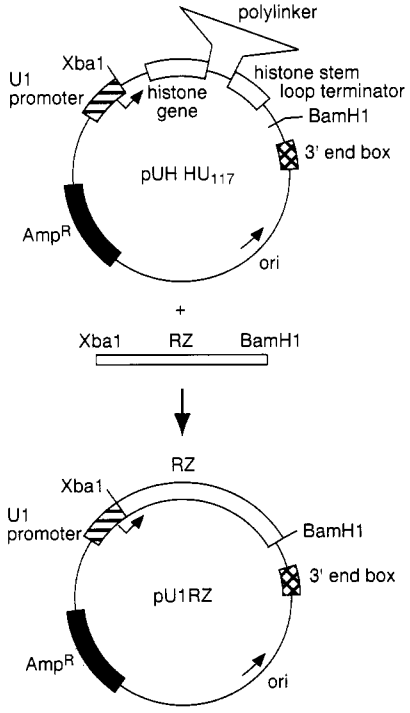

FIGURE 3: Strategy for the construction of pU1RZ from pUH HU_{117}. pUH HU_{117} was digested with *Xba*I and *Bam*HI, and the insert was separated by gel electrophoresis. A synthetic oligodeoxynucleotide duplex encoding a ribozyme (RZ) and containing *Xba*I and *Bam*HI overhangs was then ligated with the digested plasmid backbone to yield pU1RZ.

Little or no transcription was detected for constructs not beginning with a G, except for ribozyme H. The sequences of the coding strands of each ribozyme including their 5′ and 3′ arms, but without flanking sequences, are shown in Table 1.

Ribozyme Gene Cloning. Synthetic oligodeoxynucleotide duplexes encoding the desired ribozyme (minus the base(s) underlined in Table 1), as well as a 5′ *Xba*I and a 3′ *Bam*HI restriction site, were cloned into the pU1 plasmid, to yield pU1RZ (Figure 3). pU1 was prepared from pUH HU_{117} (kindly provided by W. Marzluff, Florida State University) by restriction with *Xba*I and *Bam*HI to remove the histone-coding region and termination sequences (Pilch & Marzluff, 1991) (Figure 3). *Escherichia coli* (DH5α) cells were transformed with pU1RZ, and the plasmid DNA was isolated and either used directly for nucleotide sequencing or purified over two CsCl gradients before use in transfection experiments.

Synthetic duplexes encoding the T7 promoter, the desired ribozyme, and the T7 termination sequences (Figure 2b) were also cloned between *Eco*R1 and Asp 718 sites of pSP64 (Promega, Madison, WI), which had been modified to contain an Asp 718 site, 5′ to the *Sma*I site in the multiple cloning site. The upper strand of each duplex contained linker regions [AGCAT, corresponding to the native T7 sequence (Studier et al., 1990); AAGCTT, the *Hin*dIII site; or AAT; designated as A–C, respectively, in Figure 2b] immediately 3′ to the ribozyme sequence. The linker regions were varied to avoid formation of unfavorable RNA secondary structure as predicted by MFOLD 2.2 (see below) or to introduce a *Hin*dIII restriction site. The lower strand sequence was complementary to the T7 terminator (Studier et al., 1990) and, additionally, contained sequences complementary to the respective linkers (Figure 2b). Before cloning, duplexes were prepared by annealing and then ligating the five oligonucleotides. The resulting product, purified on a 6% polyacrylamide gel, was then ligated into modified pSP64, to yield pSP64RZ. Ribozymes could be expressed from pSP64RZ in eukaryotic cells by cotransfection with pAR3126, which encodes T7 RNA polymerase (Dunn et al., 1988).

PCR To Prepare Transcription Templates from pU1RZ Constructs. Since *in vitro* transcription of the RNA polymerase II-activated U1 promoter is problematic (Gunderson et al., 1990), a PCR approach was used to produce chimeric DNA, which encoded the T7 promoter, the U1 initiation sequence, and the ribozyme and U1 termination sequences, from pU1RZ. This PCR product was then used as a template to allow T7 polymerase-mediated *in vitro* transcription, to express ribozymes with U1 initiation and termination sequences. These constructs were used for initial *in vitro* testing of catalytic activity. The 5′ PCR primers (5′-TAATACGACTCACTATAGATACTCTAG-3′ followed by either AGGCAT, CACTGT, ATCTTC, or TCAATC for ribozymes directed at sites B, H, I, and J, respectively) contained the sequence for the T7 promoter (italics), a G (single underlined) required for efficient T7 polymerase transcription, and nine bases of the U1 gene (double underlined). The 3′ primer (5′-TCAGGGGAGGCGCAACGCA-3′) was complementary to the U1 terminator site.

PCR was performed using 1 ng of each pU1RZ plasmid, 10 pmol of each primer, deoxynucleotide triphosphates (200 μM of each base), and 2.5 units of Taq polymerase in a standard buffer containing 10 mM $MgCl_2$. The amplification profile, run for 25 cycles, consisted of 1 min at 94 °C, 2 min at 55 °C, and 3 min at 72 °C. The size of the PCR product was determined by gel electrophoresis, and the remainder of the reaction was used for *in vitro* transcription.

RNA Transcription with T7 RNA Polymerase. Ribozymes were transcribed using the MegaScript T7 kit (Ambion, Austin TX). The DNA template was either one of the ribozyme "minigenes" (100 nM) (Figure 3a), the *Eco*RI/Asp 718 insert from a pSP64 ribozyme construct (100 nM) (Figure 2b), or in some instances pSP64RZ (1 ug) or one-third of the T7 promoter/U1 ribozyme PCR product described above. To aid in product detection and to determine yield, 10 μCi of

[α-^{35}S]ATP was added to each 20 μL of reaction mix. Reaction products were purified by gel electrophoresis (20% polyacrylamide/7 M urea), detected by UV shadowing or autoradiography, and extracted from the gel and precipitated in ethanol with glycogen as a carrier. Samples of the original reaction mixtures and the resuspended purified product were counted for radioactivity in a Beckman LS 6000IC scintillation counter using EcoScint A scintillation fluid (National Diagnostics, Atlanta, GA). Yield was determined as the fraction of radioactivity incorporated, multiplied by the theoretical yield. Final yields varied between 0.5 and 10 μg, depending on the template.

Determination of Ribozyme Kinetic Parameters. The kinetics of ribozyme cleavage were determined using short RNA substrates synthesized chemically by Oligoes Etc. (Wilsonville, OR). The sequences of the substrates were as follows (from 5′ to 3′): B, AUGAGGUCAUGCC; F, GGUGUGUCACACAGCUUG; H, CCCGUAUACAGUG; I, GCCGGUAGAAGAU; J, GGGGUAGGAUUGA. To determine the specificity of cleavage, reactions were also perfomed with ribozyme I_{U7C} (see below), using substrates with various mismatches (italicized) as follows: (1) GCC*U*-GUAGAAGAU; (2) GCC*U*GUAGA*U*GAU; (3) *CCCU*-GUAG*GU*GAU. RNA substrates were trace-phosphorylated with 10 μCi of [α-^{32}P]ATP (DuPont-NEN) using T4 polynucleotide kinase (USB, Cleveland, OH) for 30 min at 37 °C. Following gel purification on a 20% polyacrylamide/7 M urea gel, the concentration of each substrate was determined on the basis of the radioactivity incorporated, assuming a 100% reaction and using the known ratio of added [α-^{32}P]ATP to RNA.

Various concentrations of each RNA substrate were incubated with the corresponding ribozyme under conditions of substrate excess. Reactions were performed at 37 °C in a buffer consisting of 100 mM KCl, 10 mM $MgCl_2$ and 25 mM Tris, pH 8.0. Ribozyme concentration was typically 5 nM. Substrate concentrations varied from 10 nM to 10 μM, depending on the K_m of the ribozyme. Substrate concentrations were established to give points on the linear region of the reaction curve for each ribozyme. Aliquots of the reaction mixture were sampled at times between 15 s and 2 h, depending on ribozyme activity. The kinetics of wild-type and mutant ribozymes were compared within the same experiment. Reactions were stopped by addition of formamide-containing stop solution. Cleavage products were separated from substrate by electrophoresis on a 20% polyacrylamide/7 M urea gel. The extent of ribozyme cleavage was determined by quantitating the radioactivity in substrate and product bands, using a PhosphorImager.

Initial velocities determined from the PhosphorImager data were plotted versus the substrate concentration, and kinetic parameters were estimated using a nonlinear, least squares computer fitting program based on the Michaelis–Menten equation (KaleidaGraph, Synergy Software, Reading, PA).

Measurement of Substrate Binding by Inactive Ribozyme. Binding of ribozyme $I_{U7C,G5C}$ was determined using the method of Pyle et al., (1990). Ribozyme and ^{32}P-phosphorylated substrate were incubated together under typical reaction conditions, followed by addition of 5% glycerol and 0.01% bromphenol blue, and were then subjected to electrophoresis on a native 20% polyacrylamide gel containing 0.5× TBE with 10 mM $MgSO_4$. The radioactivity of substrate versus ribozyme:substrate complex was determined using a PhosphorImager.

RNA Structure Prediction. Conformational predictions of ribozymes, with or without added U1 or T7 sequences, were determined using MFOLD 2.2 (Jaeger et al., 1990), kindly provided by M. Zuker (Institute for Biological Sciences, National Research Council of Canada). Calculations with standard parameters were performed on a Silicon Graphics 4D/35 computer. Suboptimal forms within 10% of the energy of the optimal form were considered possible alternative structures. The structures of ribozyme sequences were modeled alone and with substrate (Konings et al., 1994). As RNA sequences are analyzed as a single strand by the program, substrate sequences were expressed as part of the ribozyme strand, separated by eight bases, designated as nonhybridizing.

Cloning of the rANF Gene for Expression in Cells. The rat ANF cDNA, previously described, was removed from pBluescriptKSrANF by *Xho*I digestion and ligated to the *Xho*I site of pREP8 (Invitrogen, San Diego, CA) for expression from the RSV promoter. The directionality and sequence of the clone were verified. The plasmid was prepared on a large scale and purified over two CsCl gradients for transfection experiments.

Cotransfection of COS-1 Cells with ANF and Ribozyme-Coding Plasmids. COS-1 cells expressing ANF mRNA transiently after transfection with pREP8rANF were used as a model system to evaluate ribozyme-mediated cleavage, since no cell lines expressing ANF mRNA stably are currently available, and cultured cardiac myocytes are difficult to transfect. COS-1 cells obtained from the American Type Culture Collection (Rockville, MD) were grown in DMEM with 10% fetal calf serum (BioWhittaker, Walkersville, MD) and standard antibiotic concentrations. The cells were split into six-well dishes (35 mm^2 per well) the day before transfection, to a density of 1×10^5 cells per well. A DNA/liposome mixture was prepared using 30 μL of DOTAP (Boehringer Mannheim) and 5 μg of plasmid DNA in 170 μL of Hepes-buffered saline. The plasmids were mixed in a molar ratio of 10:1 for pU1RZ:pREP8rANF or 10:10:1 for pSP64RZ:pAR3126:pREP8rANF. Control wells were transfected with the same plasmid ratios, with cloning vector alone, substituting for pU1RZ or pSP64RZ. Each ribozyme was transfected in duplicate. After a 10-min preincubation at room temperature, the liposome/DNA mixture was added to freshly fed cells for 6 h. After the cells were washed and the medium was changed, the cells were grown for 48–72 h before being harvested. At that time, the cells were trypsinized and centrifuged at 10000*g* for 3 min, the supernatant was removed, and the cell pellet was frozen in liquid N_2. Cell samples were stored at −80 °C until assayed for ANF mRNA content.

RNase Protection Assay for Determining Cellular ANF mRNA. Frozen cell pellets were assayed according to the method of Thompson and Gillespie (1987). Forty-five microliters of a 4 M guanidinium isothiocyanate, 25 mM sodium citrate (pH 7.0), and 0.5% *N*-laurylsarcosine solution was added to solubilize the cells. A full-length rANF antisense probe was prepared by transcribing *Eco*RI-cut pBluescript rANF with T7 RNA polymerase, using the MaxiScript system (Ambion, Austin, TX). A human β-glyceraldehyde-3-phosphate dehydrogenase (β-GAPDH) antisense probe was also prepared from pTRI-GAPDH (Ambion, Austin, TX) with T7 RNA polymerase. Both probes were internally labeled with 50 μCi of [α-^{32}P]GTP (DuPont-NEN). Each probe (5×10^5 cpm)was added to samples of the cell extract and hybridized at 37 °C overnight.

Five hundred microliters of digestion solution [20 units/mL RNase T1 (Calbiochem, LaJolla, CA), 20 μg/mL RNase

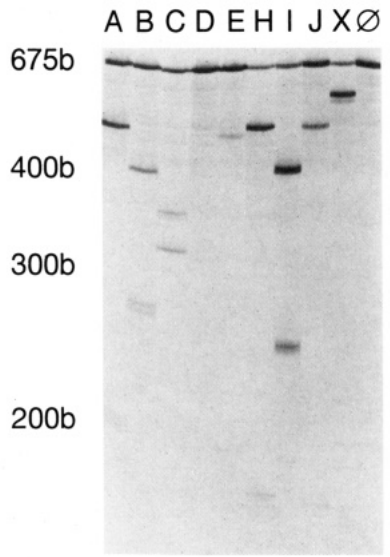

FIGURE 4: RNase H-mediated cleavage of ANF mRNA to determine target acessibility (see text for details). The ^{35}S-labeled ANF mRNA fragment (~675 nt) and smaller cleavage products are shown. Lanes A-Ø show RNase-mediated cleavage of the ANF mRNA fragment incubated in the presence of oligodeoxynucleotides directed at sites A–X (Figure 1b) or in the absence of oligodeoxynucleotide (Ø). The migration positions of 200–675-nt (b) markers are shown on the left.

Table 2: Accessibility of ANF mRNA to Oligodeoxynucleotide Binding and RNase H Cleavage

target type site	% cleavage[a]
GUC	
A	59 ± 5
B	45 ± 5
C	40 ± 3
D	22 ± 3
E	42 ± 7
GUA	
H	60 ± 3
I	71 ± 2
J	42 ± 4
translation start	
X	54 ± 4

[a] Results are the mean ± SE of 5–9 experiments for each site.

A (USB, Cleveland, OH), 0.3 M NaCl, 10 mM $MgCl_2$, and 10 units/mL DNase] was added to each hybridization mixture. This was incubated an additional 30 min at 37 °C. SDS and proteinase K were added to final concentrations of 0.4% (w/v) and 0.4 mg/mL, respectively, and the mixture was incubated for an additional 30 min at 37 °C. The mixture was extracted with 1:1 phenol/chloroform. Ten micrograms of glycogen carrier was added, and the remaining RNA was precipitated with an equal volume of 2-propanol. Genomic DNA, which immediately precipitated, was spooled prior to centrifugation in order to facilitate resuspension of nucleic acids. After centrifugation, the pellet was dried and resuspended in formamide-containing stop solution. Samples were subjected to electrophoresis using a 0.4 mm, 6% polyacrylamide gel, and the results were analyzed using a PhosphorImager.

RT-PCR To Detect Ribozyme Expression by Cells. For analysis of ribozyme expression, total RNA was purified from cell samples according to the method of Chomcynski and Sacchi (1987). Frozen cell samples (2.5×10^5 cells) were resuspended in a mixture of guanidinium isothiocyanate, sodium citrate, and *N*-laurylsarcosine and extracted with an acid/phenol solution. Nucleic acids were precipitated from the aqueous phase with ethanol and resuspended in 20 μL of 10 mM Tris, pH 7.5, 10 mM $MgCl_2$, 1 mM DTT, and 10 units of RNase inhibitor for digestion with 10 units of DNase. Following a second phenol extraction and precipitation, DNA was made from purified RNA using reverse transcriptase with standard nucleotide concentrations. Twenty-five cycles of PCR were performed as described previously. The primers for detecting expression from pU1RZ constructs were the same as those used for preparing transcription templates. Primers for detection of all T7 constructs were 5′-CTGA-(C/T)GAGGCCGAAAGGC-3′ and 5′-AAAAAACCCCT-CAAGACCC-3′. Expected PCR product sizes were 120 bp for pU1RZ constructs and 75 bp for pSP64RZ constructs. PCR products were visualized on a native polyacrylamide gel stained with ethidium bromide.

Detection of Ribozyme Activity in RNA Purified from Transfected COS Cells. RNA purified from cell extracts (above) was also incubated with phosphorylated short ribozyme substrates to detect activity of intracellularly synthesized ribozymes. These substrates were prepared as for the kinetics experiments and incubated overnight at a concentration of 100 nM with cellular RNA at 37 °C in 10 μL of standard buffer. The extent of substrate cleavage was determined by electrophoresis and autoradiographic analysis.

RESULTS

ANF mRNA Target-Site Accessibility. The nucleotide sequence of ANF mRNA was scanned for GUC and GUA sequences (Figure 1b). Sites A and H were in the region of the mRNA encoded by exon 1 of the ANF gene (Rosenzweig & Seidman, 1991); sites I, B–E, and J were in the region encoded by exon 2; and site F was in the 3′ noncoding region. Site I was ~36 bases from the region of the mRNA corresponding to the exon 2 acceptor site.

The accessibility of potential ribozyme targets on ANF mRNA, produced by in vitro transcription without a poly(A) tail, was evaluated by RNase H-directed cleavage, using oligodeoxynucleotides complementary to the mRNA target sites. Since RNase H cleaves the RNA of RNA·DNA hybrids, cleavage of ANF mRNA occurs only with binding of the oligonucleotides and, thus, reflects target-site accessibility. As shown in Figure 4 and Table 2, there were marked differences in target-site accessibility, with site D being the least accessible and site I being the most accessible. A similar pattern of accessibility for sites H, I, J, and B was also observed for cleavage of the full-length ANF mRNA by incubation with the respective *in vitro* transcribed ribozymes (data not shown). Site X at the translation start site was moderately accessible (Table 1).

Design and Kinetic Analysis of Ribozymes. On the basis of the accessibility data, ribozymes were designed to cleave sites H, I, J, and B. A ribozyme to site F was also developed, since this site is in the 3′ non-coding region and, thus, is less likely *in vivo* to be inaccessible due to protein binding. The lengths of the ribozyme arms complementary to the mRNA target sites were selected to be 5–7 bases, since in pilot studies we found that binding energies corresponding to these arm lengths gave optimal catalytic activity for ribozymes directed at several targets. The sequences of the ribozyme arms, as transcribed from the coding strands, are shown in Table 1, and examples of MFOLD 2.2-predicted optimal and first suboptimal structures, i.e., structures within 10% of the energy of the optimal forms, are shown in Figure 5. Only the optimal structure is shown for ribozyme F, since the energy state of the first suboptimal structure is >3 kcal higher than that of the optimal structure. As shown in Figure 5, in the absence

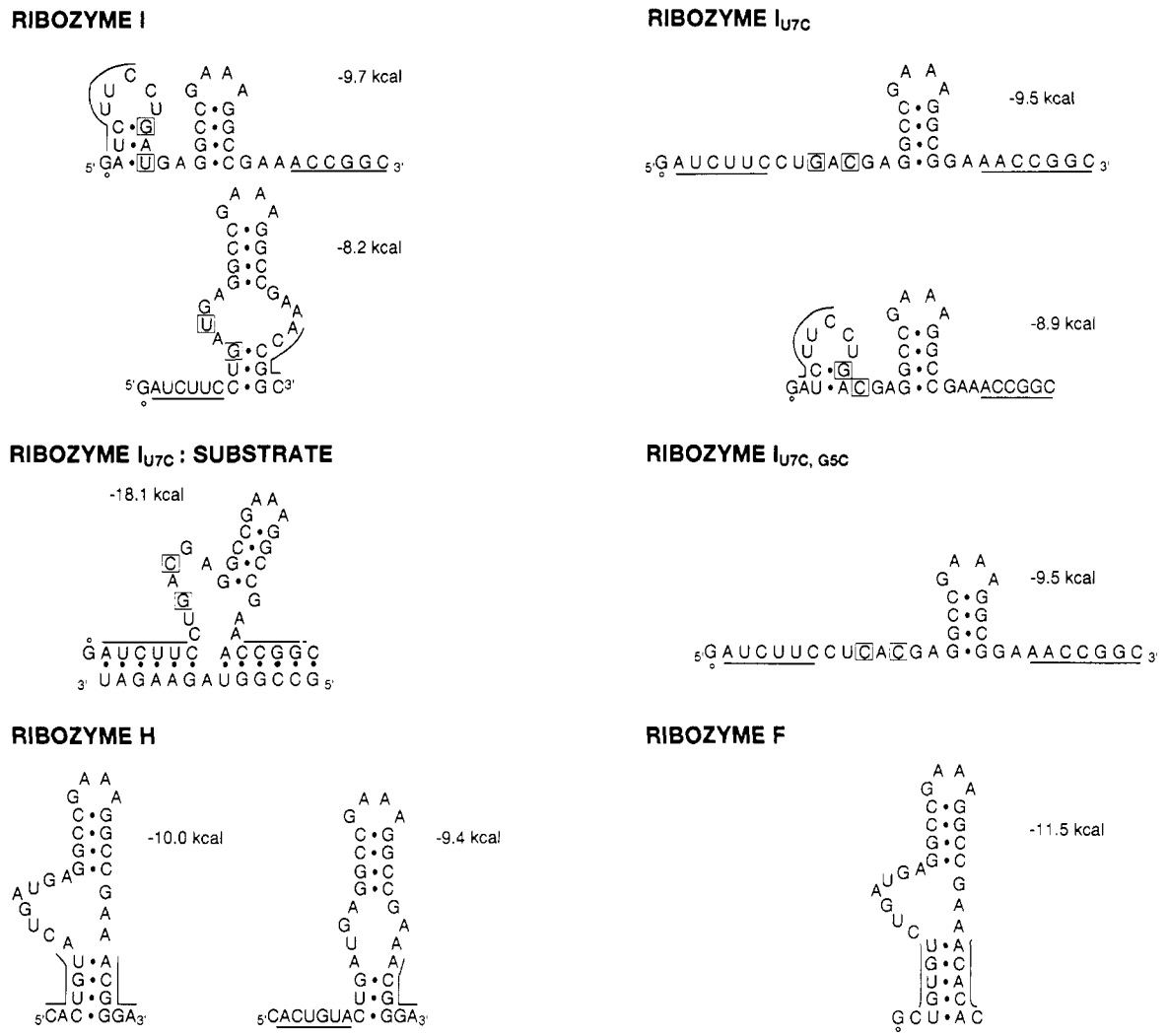

FIGURE 5: Predicted structures of ribozymes I, I_{U7C}, $I_{U7C,G5C}$, H, and F determined using MFOLD 2.2, in the absence of substrate, and for ribozyme I_{U7C} in the presence of substrate. The calculated free energies are indicated for each structure. For ribozymes I, I_{U7C}, and H the first suboptimal structures are also shown (see text for details). The O indicates that this nucleotide was added to allow efficient transcription by T7 polymerase. Nucleotides over- or underlined correspond to the ribozyme arms. The boxed nucleotides were mutated in I_{U7C} or $I_{U7C,G5C}$.

of substrate the ribozyme arms were frequently predicted to be unavailable for hybridization, and the catalytic core structures, to be unformed due to intraribozymal interactions. However, in all cases appropriate structures were predicted when the ribozymes were modeled in the presence of substrate (Figure 5). Ribozyme B (not shown) gave the most open structure, analogous to the lowest energy form of ribozyme I_{U7C} (Figure 5).

An example of RNA-substrate cleavage by ribozyme B is shown in Figure 6a. The calculated k_{cat}/K_m values for ribozymes H, I, J, B, and F, representing the pseudo-first-order rate constants for binding and cleavage, are given in Table 3. The poor catalytic efficiency of ribozyme F correlates with a K_m in the micromolar range compared to values of 10–100 nM for the other unmodified ribozymes. Ribozyme I showed no appreciable catalytic activity. Since analysis of this ribozyme structure by MFOLD 2.2 suggests an interaction between its arms and the catalytic core, base 7 [nomenclature of Hertel et al. (1992)] of the catalytic core was mutated from a U to a C, to yield ribozyme I_{U7C}. This resulted in a predicted structure in which the 5′ arm was now available for interaction with its complementary RNA target and a marked increase in catalytic activity (Table 3). An additional mutant, involving a change of base 5 from G to C in ribozyme I_{U7C}, to yield ribozyme $I_{U7C,G5C}$, was constructed to produce a structure that could still bind but was catalytically inactive (Ruffner et al., 1990). The predicted structure of ribozyme $I_{U7C,G5C}$ was unaltered from that of ribozyme I_{U7C} (Figure 5). However, this ribozyme was, indeed, unable to cleave its RNA substrate. Ribozyme-mediated cleavage was sensitive to changes in substrate composition. A substrate with a single base mismatch could be cleaved by a 3-fold excess of ribozyme, but introduction of two or four mismatches inhibited ribozyme-mediated cleavage (Figure 6b).

The influence of ionic concentration, Mg^{2+} concentration, and pH on ribozyme-mediated cleavage was also examined. As shown in Figure 7, altering the composition of the reaction buffer to that found intracellularly (100 mM KCl, pH 7.1, and 1 mM $MgCl_2$) markedly decreased the initial rate of substrate cleavage. However, with time the extent of cleavage was not markedly influenced. In more detailed kinetic studies of substrate cleavage with ribozyme J, k_{cat}/K_m values of 40, 0.1, and 0.001×10^6 M^{-1} min^{-1} were observed with reactions performed in the presence of 100 mM KCl, 20 mM Tris-HCl, pH 8.0, and 10, 5, or 1 mM $MgCl_2$, respectively. K_m increased and k_{cat} decreased as the Mg^{2+} concentration was decreased in these experiments, consistent with a role for Mg^{2+} in both binding and catalysis (Lehman & Joyce, 1993).

Influence of Flanking Sequences on Ribozyme Activity. Intracellular transcription and termination of ribozymes from

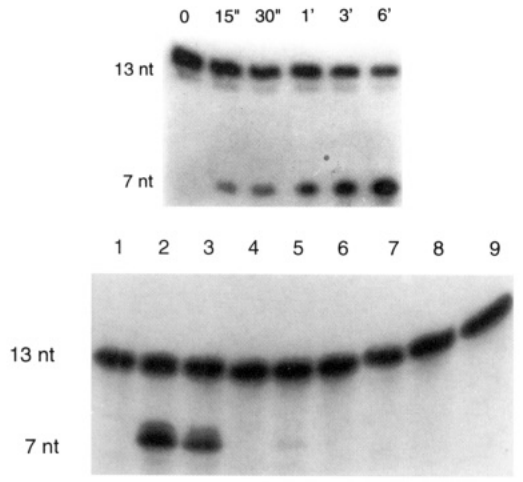

FIGURE 6: (a, upper panel) Cleavage of ^{32}P-labeled RNA substrate by ribozyme B for the times indicated. The autoradiogram shows the 13-nt substrate and the ~7-nt products. The cleavage reaction shown was performed for the times indicated, as described in Materials and Methods using 5 nM ribozyme and 25 nM substrate. The cleavage reaction shown was quantitated by PhosphorImager analysis, and the data were used to determine kinetic parameters as described in Materials and Methods. (b, lower panel) Cleavage of ^{32}P-labeled RNA substrates with one, two, or four base mismatches, with sequences as detailed in Materials and Methods, by ribozyme I_{U7C} or ribozyme U1-I_{U7C}. Lanes 1, 4, and 7, controls showing 13-nt substrates with one, two, or four base mismatches, respectively. Lanes 2 and 3, 5 and 6, and 8 and 9, cleavage of substrates with one, two, or four base mismatches, respectively, by ribozyme I_{U7C}, showing cleavage only of the substrate with a one-base mismatch to yield a 7-nt product (lanes 2 and 3). In lanes 2, 5, and 8 the substrates were incubated with ribozyme I_{U7C} transcribed from an oligonucleotide cassette (see Materials and Methods). Ribozyme U1-I_{U7C} used in lanes 3, 6, and 9 was transcribed with T7 RNA polymerase from a PCR-generated template prepared from the U1-I_{U7C} plasmid, as described in Materials and Methods.

Table 3: Kinetics of Ribozyme Cleavage

ANF mRNA target sites	k_{cat}/K_m($\times 10^6$ M^{-1} min^{-1})
native ribozymes	
B	75
F	1
H	11
I	n.d.[a]
I_{U7C}[b]	16
$I_{U7C,G5C}$[c]	n.d.
J	40
U1 ribozymes[d]	
U1-B	0.07
U1-H	1.3
U1-I_{U7C}	1.3
U1-J	120
T7 ribozymes[e]	
B-$T7_C$	0.4
H-$T7_A$	16
H-$T7_C$	1.5
I_{U7C}-$T7_A$	7.6
J-$T7_B$	22

[a] n.d., not determinable; no substrate cleavage was observed with these ribozymes. [b] Ribozyme I with U → C mutation of base 7. [c] Ribozyme I_{UC} with G → C mutation of base 5. [d] Native ribozymes with addition of U1 flanking sequences. [e] Native ribozymes with addition of a T7 terminator coupled by various linker sequences (A–C) (Figure 10).

either the U1 or the T7 promoter required that additional sequence be added 5′ and 3′ of the ribozymes. Ribozymes expressed from the pU1 vector system contained nine bases of U1 initiation sequence, including a restriction site, located 5′ to their 5′ arms and 61 bases 3′ to their 3′ arms that are required for termination of transcription. Ribozymes expressed from the pSP64 (T7) vector system were modified by addition of a T7 terminator preceded by linker A, B, or C (see Materials and Methods and Figure 10a).

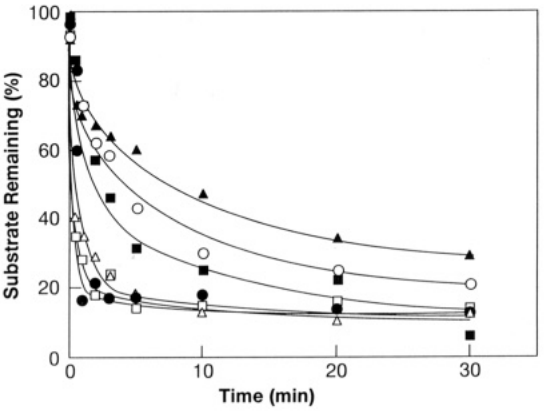

FIGURE 7: Effect of Mg^{2+} concentration and pH on ribozyme-mediated cleavage of RNA substrate. Ribozyme J and its RNA substrate were incubated in a 1:1 molar ratio, and cleavage was determined as detailed in Materials and Methods. The compositions of the reaction media were as follows: □, 0 mM KCl, 20 mM $MgCl_2$, and 75 mM Tris-HCl, pH 8.0; ●, 0 mM KCl, 10 mM $MgCl_2$, 75 mM Tris-HCl, pH 8.0, 1.2 mM spermidine; △ 0 mM KCl, 10 mM $MgCl_2$, and 75 mM Tris-HCl, pH 8.0; ■, 100 mM KCl, 10 mM $MgCl_2$, and 20 mM Tris-HCl, pH 8.0; ○, 100 mM KCl, 10 mM $MgCl_2$, and 20 mM Tris-HCl, pH 7.1; ▲, 100 mM KCl, 1 mM $MgCl_2$, and 20 mM Tris-HCl, pH 7.1.

MFOLD2.2 was used to predict whether added U1 or T7 sequences were likely to interfere with ribozyme structures and, hence, activity. Examples of the predicted structures of the ribozymes and U1 flanking sequences are shown in Figure 8. Although unfavorable structures were predicted in the absence of substrate, modeling of the U1-ribozyme structures in the presence of substrate suggested that appropriate catalytic structures would form. The catalytic activity of these ribozymes is given in Table 3. Ribozymes U1-B, U1-H, and U1-I_{U7C} show reduced catalytic activity compared to the native ribozymes. This may be due to the formation of alternative structures involving the U1 flanking sequences. However, the k_{cat}/K_m of ribozyme U1-J was enhanced over that of ribozyme J. Correspondingly, no change in ribozyme structure was observed with the added sequence (Figure 9).

Modeling of ribozyme H, I_{U7C}, and J structures with the addition of the T7 terminator revealed no potentially unfavorable interactions and particularly no hybridizations of the 3′ arms with the linker or terminator region. Ribozyme B modeling showed potentially unfavorable structure with linker A or B, so linker C was used. As shown in Table 3, as compared to the native ribozymes, the addition of the linker and T7 flanking sequences diminished catalytic activity. An observed increase in K_m suggests that the addition of the bulky T7 terminator destabilizes the ribozyme–substrate interaction, presumably due to reduced or slowed binding by the 3′ arms. Utilization of linker C appears to reduce catalytic activity even further. The catalytic activity of ribozyme B-T7 was markedly less than that observed for native ribozyme B (Table 3). Poor catalytic activity was also observed for ribozyme H-$T7_C$ as compared to ribozyme H-$T7_A$ (Table 3).

The structure of the linker region between ribozyme and T7 terminator appears to be critical for termination since little, if any, of the expected 104-nt transcript was observed with *in vitro* transcription of ribozyme J-$T7_B$ in pSP64, versus ribozyme B-$T7_C$ or I_{U7C}-$T7_A$ in pSP64 (Figure 10b). Failure of the transcript from pSP64J-$T7_B$ to terminate resulted in a 430-nt structure (Figure 10b). *In vitro* this extended

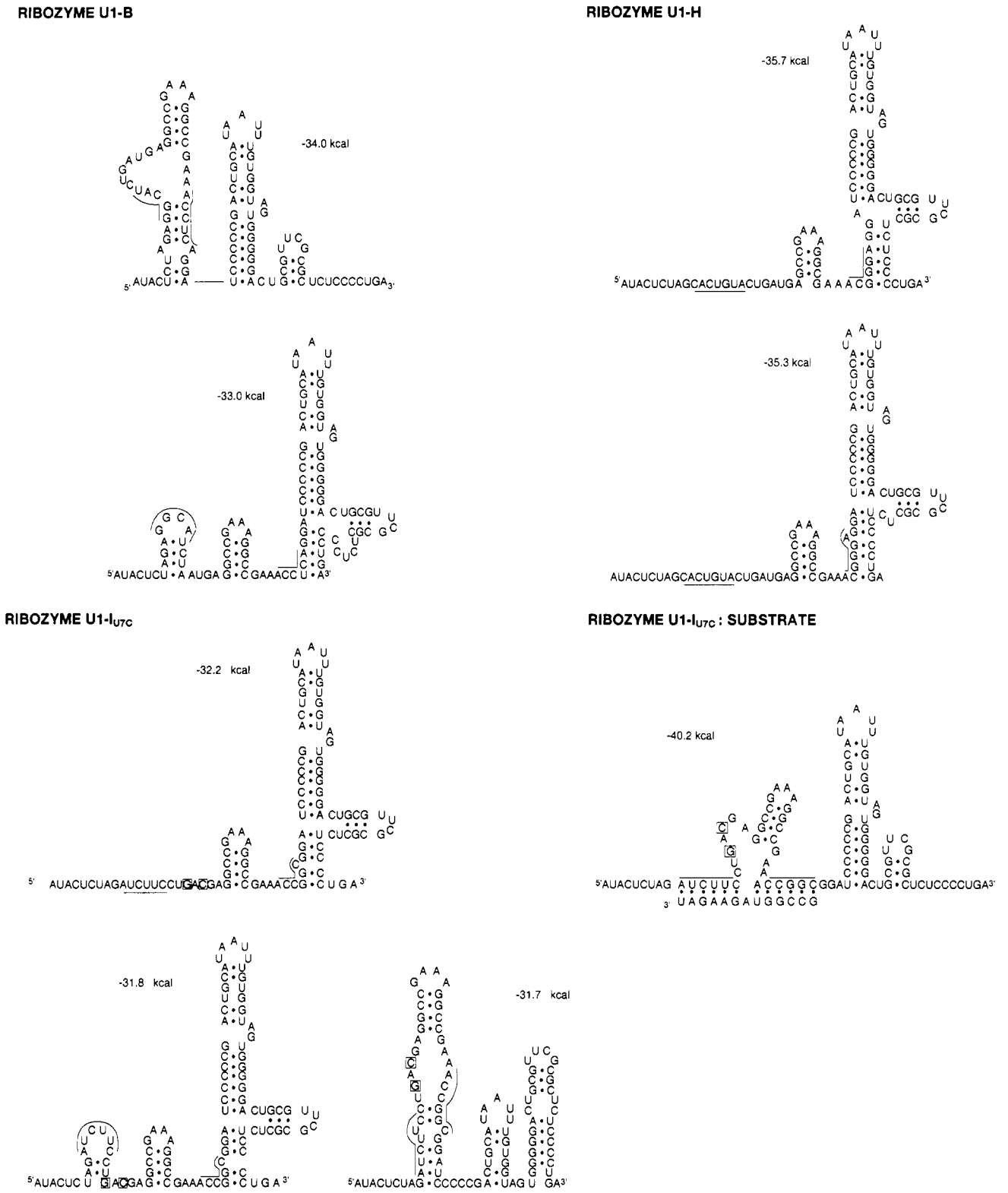

FIGURE 8: Predicted structures for ribozymes U1-B, U1-H, and U1-I_{U7C} determined using MFOLD 2.2 in the absence of substrate and for ribozyme U1-I_{U7C} in the presence of substrate. For ribozymes U1-B, U1-H, and U1-I_{U7C} the first or alternative suboptimal structures are also shown (see Figure 5 and text for details and symbols).

ribozyme structure cleaved 30% less substrate than the 104-nt structure produced by transcription of pSP64J-$T7_B$ after initial digestion of the plasmid at a restriction site (Asp 718) immediately 3′ to the T7 terminator (ribozyme J-$T7_B$, Table 3).

Ribozyme U1-$I_{U7C,G5C}$, intended to bind but to be inactive (Ruffner et al., 1990), was also examined for catalytic activity. As expected, only trace amounts of substrate cleavage were observed after incubation of a 3-fold excess of ribozyme over substrate for 3 h at 37 °C. To verify that ribozyme U1-$I_{U7C,G5C}$ indeed binds substrate, it was incubated with substrate under the same conditions in a molar ratio of approximately 1:1, and hybridization was evaluated by non-denaturing gel electrophoresis (see Materials and Methods). Under these conditions almost 50% of the substrate was bound (data not shown).

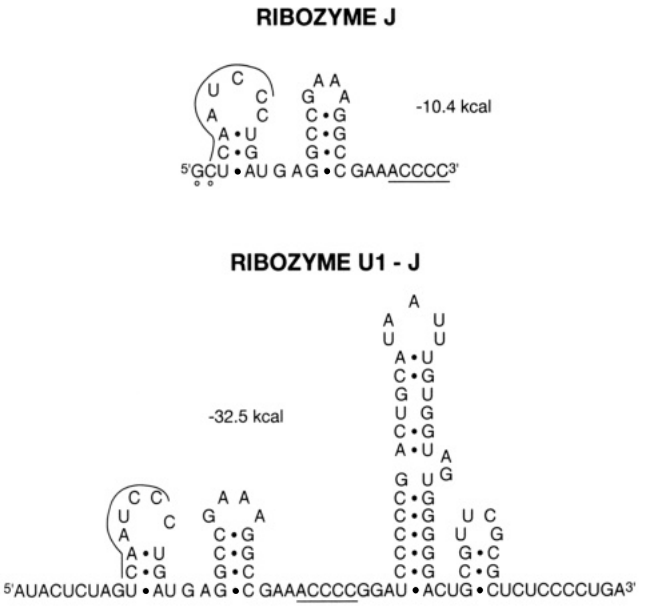

FIGURE 9: Predicted structures of ribozymes J and U1-J (see Figure 5 and text for details).

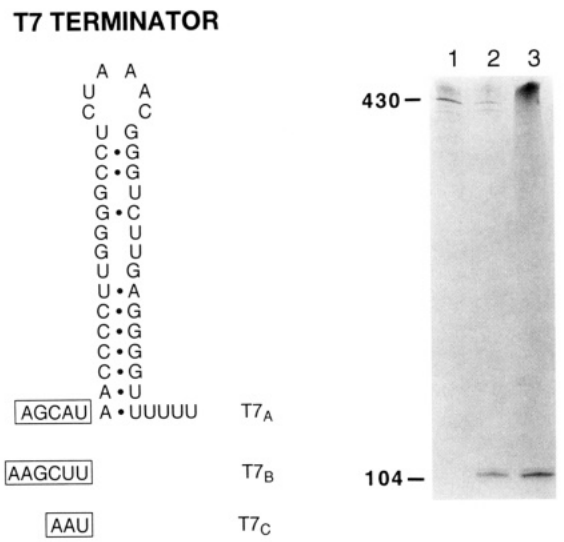

FIGURE 10: (a) Predicted structure of the T7 terminator and linkers A, B and C. (b) Products of *in vitro* transcription of *Sph*I-digested pSP64RZJ-$T7_B$ (lane 1), pSP64RZI_{U7C}-$T7_A$ (lane 2), and pSP64RZB-$T7_C$ (lane 3) using T7 polymerase. Termination of transcription immediately 3′ to the T7 terminator results in a 104-nt ribozyme, whereas failure to terminate at this site results in 430-nt transcript.

Intracellular Activity of Expressed Ribozymes. To examine the activity of ribozymes *in vivo,* COS-1 cells were cotransfected with the ribozyme-encoding plasmids, as well as with pREP8rANF. For analysis of the U1 constructs, cells were cotransfected with pREP8rANF and the various pU1RZ constructs. As shown in Figure 12, whereas the expression of β-GAPDH mRNA remained constant, ANF mRNA decreased markedly in the cells expressing ribozyme U1-I_{U7C}, U1-H, and U1-B. The catalytically inactive ribozyme U1-$I_{U7C,G5C}$ also decreased ANF mRNA, probably due to an antisense effect, but this decrease was less than that observed with ribozyme U1-I_{U7C} (Figure 12). For the experiments shown in Figure 12, ANF mRNA, relative to β-GAPDH and normalized to 0% for cells transfected only with pU1RZ plasmids, decreased by an average of 92%, 95%, 97%, 77%, and 60% in cells expressing ribozymes U1-B, U1-H, U1-I_{U7C}, U1-$I_{U7C,G5C}$, and U1-J, respectively. Similar results were obtained in three additional experiments performed in duplicate, and in all studies the ribozymes directed at sites H and I were the most active. In these studies cleavage of ANF mRNA was evaluated 72 h after transfection. Similar degrees of ANF mRNA cleavage were also observed 48 h after transfection, as shown, for example, for ribozymes U1-I_{U7C} and U1-$I_{U7C,G5C}$ (Figure 12).

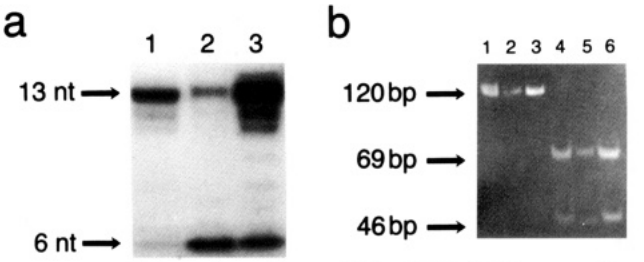

FIGURE 11: (a) Detection of intracellular ANF mRNA expression by *in vitro* cleavage of RNA substrates. Total RNA was purified from COS-1 cells transfected with pREP8rANF alone (lane 1, control), with pREP8rANF plus pU1RZH (lane 2), or with pREP8rANF plus pSP64ZH-$T7_A$ (lane 3) and tested *in vitro* for cleavage of RNA substrate, as described in Materials and Methods. ^{32}P-Labeled substrate (13 nt) is seen in lanes 1–3, and product (6 nt) is seen in lanes 2 and 3. (b) Detection of expression of pU1RZ constructs by RT-PCR. Total RNA prepared from COS-1 cells transfected with pU1RZH (lanes 1 and 4), pU1RZI_{U7C} (lanes 2 and 5), or pU1RZJ (lanes 3 and 6) was treated with reverse transcriptase (RT) and then subjected to 25 cycles of PCR (polymerase chain reaction), as detailed in Materials and Methods. The resulting ethidium bromide-stained PCR products, before (120-bp products, lanes 1–3) and after digestion at two internal *Hae*III sites (69- and 46-bp products, lanes 4–6), are shown. An additional 8-bp product resulting from the *Hae*III digestion is not shown.

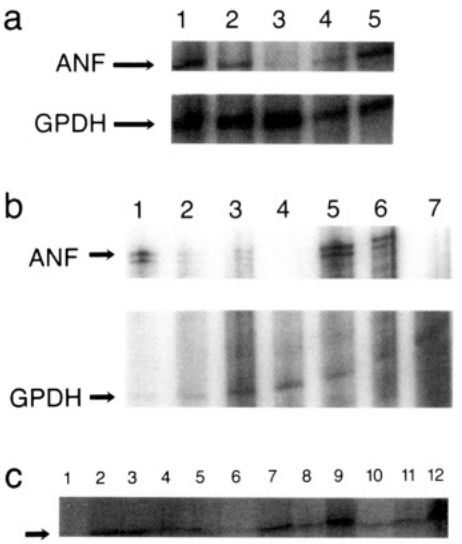

FIGURE 12: Intracellular cleavage of ANF mRNA. (a) COS-1 cells were transfected with pREP8rANF, pSP64, and pAR3126 (lane 1, control) or pREP8rANF, pAR3126, and either pSP64RZB-$T7_C$ (lane 2), pSP64RZH-$T7_A$ (lane 3), pSP64RZI_{U7C}-$T7_A$ (lane 4), or pSP64RZJ-$T7_B$ (lane 5), and ANF mRNA and GAPDH mRNA expression were determined 72 h later by RNase protection, as described in Materials and Methods. (b) ANF mRNA expression was determined as in panel a, 72 h after transfection with pREP8rANF plus pBluescript KS (lane 1, control); with pREP8rANF plus either pU1RZB (lane 2), pU1RZH (lane 3), pU1RZI_{U7C} (lane 4), pU1RZJ (lane 5), or pU1$RZI_{U7C,G5C}$ (lane 6); or with no plasmid (mock) (lane 7). (c) ANF mRNA expression was determined as in panel a, 48 (lanes 1 and 2) or 72 h (lanes 3–12) after transfection with pREP8rANF plus either pU1RZI_{U7C} (lane 1), pU1$RZI_{U7C,G5C}$ (lane 2), pU1RZJ (lane 3), pU1RZH (lane 4), pU1RZB (lane 5), pSP64$RZI_{U7C,G5C}$-$T7_A$ (lane 7), pSP64RZI_{U7C}-$T7_A$ (lane 8), pSP64RZJ-$T7_B$ (lane 9), pSP64RZH-$T7_A$ (lane 10), or pSP64RZB-$T7_C$ (lane 11); with no plasmid (mock) (lane 6); or with pREP8rANF plus pSP64 (lane 12, control).

For the T7 ribozyme constructs, cells were cotransfected with the various pSP64RZ constructs and pREP8rANF, as well as with pAR3126. pAR3126 provided T7 polymerase, which is required for expression of the ribozymes under the control of the T7 promoter. As shown in Figure 12, in these experiments ANF mRNA decreased by an average of 73%, 99%, 78%, and 0% in cells expressing ribozymes B-$T7_C$, H-$T7_A$, I_{U7C}-$T7_A$, and J-$T7_B$, respectively. Again, in four such experiments, ribozymes directed at sites H and I were the most active.

Cellular expression of ribozymes from the various pU1RZ constructs was determined by RT-PCR of total RNA prepared from the COS-1 cell transfectants. In all cases, except for cells transfected only with pREP8rANF, a PCR product of the predicted molecular weight was obtained and could be appropriately digested at an internal restriction site (Figure 11). However, with RT treatment of RNA prepared from the COS-1 cells transfected with the pSP64RZ constructs and then 25 cycles of PCR, little, if any, ribozyme expression was observed. This may have been due to the short size of the PCR product (75 nt), the low abundance of the ribozyme RNA, or the inability of the primers to hybridize to the ribozymes. To obviate this problem, cellular RNA was purified from the COS-1 transfectants and then tested for substrate cleavage *in vitro* (Figure 11). In all cases substrate cleavage could be demonstrated, as shown in Figure 12 for ribozyme H-$T7_A$. Using this approach, intracellular ribozyme expression could be similarly demonstrated for the U1 constructs (Figure 12).

DISCUSSION

Expression of ribozymes that are catalytically active *in vivo* is an important prerequisite for their use in gene inactivation, either therapeutically or for physiological studies. Several studies have been unable to show that ribozymes are significantly more active than antisense RNA (Lo et al., 1992; Saxena & Ackerman, 1990). One possible reason for this is inadequate optimization of ribozyme structure to ensure catalytic activity. Extremely long arm lengths, for example, can inhibit ribozyme activity (Goodchild & Kohli, 1991), as can the formation of alternative, unfavorable structures (Heus et al., 1990). In this study we have evaluated the use of U1 and T7 vector systems for expressing ribozymes that are catalytically active *in vivo*. In addition, we have attempted to develop favorable ribozyme constructs by evaluating variables that could influence ribozyme structure, binding, and activity.

The U1 vector system used in this study has advantages for directing the expression of short, defined transcripts in high copy number. The U1 gene is a member of a class of small nuclear RNAs (UsnRNAs) that are ubiquitously expressed under the control of a strong RNA polymerase II promoter and play an important role in the processing of precursor RNAs (Ciliberto et al., 1986). snRNAs, like histone genes, are not polyadenylated. In addition to a potential stem and loop structure at the 3′ end of UsnRNAs, there is a conserved sequence [GTTTNo-$_3$AAA(G/A)NNAGA, the 3′ end box] in the immediate 3′ flanking region (Hernandez, 1985). Formation of the 3′ ends of UsnRNAs involves initial extension at the 3′ ends of the transcripts by several (up to 15) nucleotides, which are then removed by exonuclease activity (Madore et al., 1984). The conserved 3′ end box is the only element absolutely required for precursor 3′ end formation (Hernandez, 1985). Thus, U1 vectors, such as pUH HU_{117}, which contains the U1 promoter and the U1 3′ end (terminator), can direct high-level expression of short, defined, stable transcripts that are not polyadenylated.

Plasmids containing target genes flanked by the vaccinia virus T7 promoter and termination sequences are also useful for producing high-level expression of RNA transcripts. The T7 terminator produces a transcript of limited and defined size and, because of its likely stem-loop structure, probably improves message stability by limiting the action of RNases. Addition of the T7 terminator seemed to have a more neutral effect on ribozyme structure and activity (Table 3) than the U1 terminator, although the linker region between the 3′ end of the ribozyme and the T7 terminator appears to be critical for proper termination of transcription (Figure 10b) and for ribozyme activity (Table 3). The T7 vector system used in this study is unsuitable for stable expression in cells. T7 polymerase, required for T7-promoter-directed expression, resides exclusively in the cytoplasm (Dunn et al., 1988). This requires that pSP64RZ also be in the cytoplasm for ribozyme transcription, which would not be the case with stable transfection of pSP64RZ. Effective expression of T7 or T3 RNA polymerase in the nucleus has been achieved by the addition of a nuclear localization signal (Dunn et al., 1988; Zhou et al., 1990) and might be adapted to stable expression of ribozymes, although the difference in cellular compartmentalization might alter ribozyme activity. The advantages of the T7 or T3 systems are the high level of expression achieved with these viral polymerases and the ease with which T7 or T3 constructs can be tested *in vitro*.

RNA structure prediction, particularly of short ribozyme sequences, has the potential to aid in the design of the most active ribozymes and the structures most likely to be active in a given expression system. However, prediction of ribozyme activity from the structures modeled with MFOLD 2.2 is not straightforward. In the presence of substrate, the lowest free energy structures were always predicted to contain the correctly folded catalytic core with the flanking arms hydridizing appropriately to the target substrate. However, this prediction was inconsistent with the experimental results for ribozymes I, F, and U1-B. The poor catalytic activity of these ribozymes correlated better with their structures modeled in the absence of substrate, which predicts arms that would not be available for hybridization to substrate provided *in trans*. Conversely, ribozyme B, which was predicted to be open and able to hybridize substrate, had the highest catalytic activity. Analysis of the structure of ribozyme I was also informative, since it allowed us to deduce that the mutation of a single base would provide a more open structure, and this mutant (ribozyme I_{U7C}) was, indeed, catalytically active (Figure 5; Table 3). Nevertheless, several of the ribozymes were significantly more active than might be predicted from their MFOLD 2.2 structures. Neither the ribozyme H nor the ribozyme J structure would be expected to be active on the basis of the predicted ability of their arms to hybridize (Figures 5 and 9), although it is possible that some bases in the loop of ribozyme J can bind to substrate. Also, the structures of the predicted optimal and first suboptimal forms of ribozyme H may be close enough energetically that they are in equilibrium, allowing substrate binding during structural transition. Similarly, ribozymes U1-H and U1-I_{U7C} would appear to have significant interactions with the U1 terminator sequence, yet they are active, although less so than ribozyme U1-J. Again, these structures may be oscillating between several suboptimal forms. Overall, structural predictions with MFOLD 2.2 may be useful in avoiding or changing highly distorted ribozymes, yet ribozymes with structural imperfections may have adequate activity.

Structural prediction of larger RNA sequences such as the ANF mRNA is even less reliable. The optimal structure predicted (data not shown) did not correlate with the accessibilities observed using the RNase H cleavage assay. Sites C and E were in loop regions and almost entirely accessible in the predicted structure, but not optimally accessible to oligodeoxynucleotide binding *in vitro*. Conversely, the most accessible sites experimentally (sites H and I) were predicted to be hybridized to other bases in stem regions. L'Huillier et al. (1992) also did not find convincing correlations between sites cleaved intracellularly and predicted accessible regions in a large mRNA. Thus, the RNase H cleavage assay is a more useful means of locating accessible sites intracellularly than structure prediction, and it may aid generally in selection of suitable targets.

Ribozyme activity is likely to be altered in the cellular environment. For example, proteins may bind to portions of the RNA substrate or to the ribozyme itself, interfering with catalysis. In addition, the intracellular pH is 7.1 (Weissberg et al., 1989), whereas a more basic pH is required for optimal ribozyme activity. Although there is a significant cellular reservoir of Mg^{2+} bound to proteins, nucleic acids, and nucleotides that may become available in the cell under certain conditions, the intracellular free Mg^{2+} concentration is 0.3–1 mM (Romani & Scarpa, 1992; Murphy et al., 1991), which is far lower than required for optimal activity. Decreased catalytic efficiency in the presence of physiological free Mg^{2+} concentrations may significantly diminish the initial rate of ribozyme-mediated cleavage in cells. It may be possible to compensate for the decreases in affinity for substrate caused by a low Mg^{2+} environment by increasing the lengths of the arms hybridizing to substrate. The value of designing ribozymes with longer arms to obviate the higher K_m values under physiological conditions will be explored in future experiments. This additional optimization step may be useful when ribozymes give partial intracellular cleavage of a putatively accessible site.

Analysis of ribozyme activity in cells (Figure 11) revealed that, *in vivo*, destruction of ANF mRNA is not strictly proportional to the rate of ribozyme catalysis *in vitro*. Ribozyme U1-B, which had a high K_m and low k_{cat}, was more active when expressed in cells than ribozyme U1-J, which was the most catalytically active ribozyme *in vitro* (Table 3). Ribozymes U1-H and U1-I_{U7C} were the most active within cells, despite their diminished *in vitro* activity following expression with adjacent U1 sequences. In fact, the greatest decreases in cellular ANF mRNA were observed with ribozymes directed to site H or I, regardless of expression from the U1 system or with T7 RNA polymerase. This finding correlates with the results of the RNase H cleavage assay (Table 2), which showed that sites H and I are most accessible to oligodeoxynucleotide binding *in vitro*. This correlation suggests that mRNA structure in cells may be similar to that found *in vitro*.

As shown here, the extent of ribozyme cleavage in cells can exceed the extent of cleavage of full-length mRNA *in vitro* (Table 2 versus Figure 11). This may be due, in part, to RNases acting on the double-stranded ribozyme–RNA complex or to other mechanisms involved in antisense RNA activity. Moreover, the cellular environment may enhance ribozyme activity in several ways. First, continual synthesis of ribozymes may allow longer reaction times than those used by us *in vitro*. Second, a powerful promoter can result in significant ribozyme excess. In addition, RNases in the cell also digest reaction products, which may reduce competition for ribozyme binding. Endogenous polyamines, such as spermidine, may also partially compensate for the low intracellular Mg^{2+} concentrations by limiting target-site inaccessibility due to RNA secondary structure. Finally, cell proteins, such as the nucleocapsid protein of HIV type I, which catalyze annealing, may enhance cellular activity (Tsuchihashi et al., 1993). In addition, ribozyme cleavage in cells may be even more specific than *in vitro*. It is unlikely, on the basis of our *in vitro* data, that targets differing by two or more hybridizing bases would be cleaved by a ribozyme. Targets with a single mismatch may be cleaved, but this requires that (a) the analogous sequence be available within its RNA secondary structure and (b) the similar sequence be unbound by proteins. Thus, the cellular milieu may increase the stringency of ribozyme cleavage.

Ribozymes have been reported to be active in cells when expressed in tandem with other ribozymes (Chen et al., 1992), as part of a tRNA cassette (Yuyama et al., 1992; Yu et al., 1993), as part of a neomycin phosphotransferase gene (Steinecke et al., 1992), and when cleaved from a primary transcript by another ribozyme (Ojwang et al., 1992). Expression of ribozymes using the U1 vector system is an alternative approach that has minimal effects on catalysis and should give a naturally stable transcript. This system should be applicable not only to ANF mRNA cleavage but also to inactivation of other target genes.

ACKNOWLEDGMENT

We thank A. H. Rosenberg for pAR3126, L. Ramamurthy and W. F. Marzluff for pUH HU_{117}, M. Zucker for MFOLD2.2, J. Thompson for technical assistance, A. Husain and S. Karnik for valuable discussions, and E. Martin for expert secretarial assistance.

REFERENCES

Blaine, E. H. (1990) *Hypertension 15*, 2–8.
Cameron, F. H., & Jennings, P. A. (1989) *Proc. Natl. Acad. Sci. U.S.A. 86*, 9139–9143.
Chen, C.-J., Banerjea, A. C., Harmison, G. G., Haglund, K., & Schubert, M. (1992) *Nucleic Acids Res. 20*, 4581–4589.
Chomczynski, P., & Sacchi, N. (1987) *Anal. Biochem. 162*, 156–159.
Ciliberto, G., Dathan, N., Frank, R., Philipson, L., & Mattaj, I. W. (1986) *EMBO J. 5*, 2931–2937.
Dropulic, B., Lin, N. H., & Jeang, K.-T. (1993) *Nucleic Acids Res. 21*, 2273–2274.
Dunn, J. J., Krippl, B., Bernstein, K. E., Westphal, H., & Studier, F. W. (1988) *Gene 68*, 259–266.
Goetz, K. L. (1990) *Hypertension 15*, 9–19.
Goodchild, J., & Kohli, V. (1991) *Arch. Biochem. Biophys. 284* (2), 386–391.
Gunderson, S. L., Knuth, M. W., & Burgess, R. R. (1990) *Genes Dev. 4*, 2048–2060.
Haseloff, J., & Gerlach, W. L. (1988) *Nature 334*, 585–591.
Hernandez, N. (1985) *EMBO J. 4*, 1827–1837.
Hertel, K. J., Pardi, A., Uhlenbeck, O. C., Koizumi, M., Ohtsuka, E., Uesugi, S., et al. (1992) *Nucleic Acids Res. 20*, 3252.
Heus, H. A., Uhlenbeck, O. C., & Pardi, A. (1990) *Nucleic Acids Res. 18*, 1103–1108.
Jaeger, J. A., Turner, D. H., & Zuker, M. (1990) *Methods Enzymol. 183*, 281–306.
Konings, D., McSwiggen, J. A., & Christoffersen, R. E. (1994) *THEOCHEM* (in press).
L'Huillier, P. J., Davis, S. R., & Bellamy, A. R. (1992) *EMBO J. 11*, 4411–4418.
Lehman, N., & Joyce, G. F. (1993) *Nature 361*, 182–185.
Lo, K. M. S., Biasolo, M. A., Dehni, G., Palu, G., & Haseltine, W. A. (1992) *Virology 190*, 176–183.

Madore, S. L., Wieben, D. E., & Pederson, T. (1984) *J. Cell Biol. 98,* 188–192.
Mazzolini, L., Axelos, M., Lescuare, N., & Yot, P. (1992) *Plant Mol. Biol. 20,* 715–731.
Milligan, J. F., Groebe, D. R., Witherell, G. W., & Uhlenbeck, O. C. (1987) *Nucleic Acids Res. 15,* 8783–8798.
Murphy, E., Freudenrich C. C., & Lieberman M. (1991) *Annu. Rev. Physiol. 53,* 273–287.
Ojwang, J. O., Hampel, A., Looney, D. J., Wong-Staal, F., & Rappaport, J. (1992) *Proc. Natl. Acad. Sci. U.S.A. 89,* 10802–10806.
Pilch, D. R., & Marzluff, W. F. (1991) *Gene Exp. 1,* 41–53.
Pyle, A. M., McSwiggen, J. A., & Cech, T. R. (1990) *Proc. Natl. Acad. Sci. U.S.A. 87,* 8187–8191.
Romani, A., & Scarpa, A. (1992) *Arch. Biochem. Biophys. 298* (1), 1–12.
Rosenzweig, A., & Seidman, C. E. (1991) *Annu. Rev. Biochem. 60,* 229–255.
Ruffner, D. E., Stormo, G. D., & Uhlenbeck, O. C. (1990) *Biochemistry 29,* 10695–10702.
Saxena, S. K., & Ackerman, E. J. (1990) *J. Biol. Chem. 28,* 17106–17109.
Seidman, C. E., Duby, A. D., Choi, E., Graham, R. M., Haber, E., Homcy, C., Smith, J. A., & Seidman, J. G. (1984) *Science 225,* 324–326.
Sioud, M., Natvig, J. B., & Forre, O. (1992) *J. Mol. Biol. 223,* 831–835.
Steinecke, P., Herget, T., & Schreier, P. H. (1992) *EMBO J. 11,* 1525–1530.
Steinhelper, M. E., Cochrane, K. L., & Field, L. J. (1990) *Hypertension 16,* 301–307.
Studier, F. W., Rosenberg, A. H., Dunn, J. J., & Dubendorff, J. W. (1990) *Methods Enzymol. 185,* 60–89.
Symons, R. H. (1992) *Annu. Rev. Biochem. 61,* 641–671.
Thompson, J. D., & Gillespie, D. (1987) *Anal. Biochem 163,* 281–291.
Tsuchihashi, Z., Khosla, M., & Herschlag, D. (1993) *Science 262,* 99–102.
Weissberg, P. L., Little, P. J., Cragoe, E. J., & Bobik, A. (1989) *Circ. Res. 64,* 676–685.
Wildey, G. M., Misono, K. S., & Graham, R. M. (1992) in *The Heart and Cardiovascular System* Second Edition (Fozzard, H. A., et al., Eds.) 2nd ed., pp 1777–1796, Raven Press Ltd., New York.
Yu, M., Ojwang, J., Yamada, O., Hampel, A., Rappaport, J., Looney, D., & Wong-Staal, F. (1993) *Proc. Natl. Acad. Sci. U.S.A. 90,* 6340–6344.
Yuyama, N., Ohkawa, J., Inokuchi, Y., Shirai, M., Sato, A., Nishikawa, S., & Taira, K. (1992) *Biochem. Biophys. Res. Commun. 186,* 1271–1279.
Zhou, Y., Giordano, T. J., Durbin, R. K., & McAllister, W. T. (1990) *Mol. Cell. Biol. 10,* 4529–4537.